



Electropermanent magnet blank holder technique in sheet metal deep drawing

Siji Qin¹ · Hongsheng Zhang^{1,2} · Yaoben Mao¹ · Le Yang¹ · Xianbin Li¹ · Zonghui Hu¹ · Xiao Cheng¹

Received: 17 May 2019 / Accepted: 27 January 2020

© Springer-Verlag London Ltd., part of Springer Nature 2020 / Published online: 10 February 2020

Abstract

A novel blank holder technique based on electropermanent magnet (EPM) technology is proposed, in which independent loading of blank holding force (BHF) can be realized in sheet metal forming process. The magnetic force and the resulting BHF are applied by permanent magnets rather than electromagnets, and the current is only required at the moment of loading or unloading the BHF. The BHF is convenient in control, low in energy consumption, and without overheating problem using this technique. In this paper, an experimental setup consisting of magnetic cushion, die, punch, and other components is designed based on the characteristics of EPM and requirements of deep drawing process. The magnetic cushion including blank holder and magnetic pole units is used to generate magnetic force and realize loading and unloading of BHF. Then, magnetic field analyses of a pair of magnetic pole units and the designed cushion are carried out by FEM. Also, the coupling problem involving magnetic field and stress field is further analyzed and solved by means of theoretical method and FEM, and the BHF and the blank holding pressure on the sheet using the new technique can be obtained. The deformation of the designed setup is small, and the stiffness can satisfy the requirements. The deep drawing processes of cylindrical cup of 08Al sheet with 0.98 mm thickness are simulated by using conventional blank holder and the new technique, respectively, and there are small differences of the strain distributions of the drawn parts with the two techniques. The experiments of cylindrical cup deep drawing applied four different BHF, respectively, are carried out using EPM blank holder technique. The results indicate that the BHF applied by the designed cushion is large enough for the deep drawing process of the selected sheet.

Keywords Electropermanent magnet · Sheet metal forming · Deep drawing · Blank holder technique · Magnetic flux density · Coupling analysis

1 Introduction

In sheet metal forming process, blank holding force (BHF) is one of the most important process variables to reduce the occurrence of forming defects. Wrinkling can occur where BHF is not sufficient enough to suppress buckling of the sheet metal, while cracking will occur when the BHF is excessive due to an insufficient material flow [1, 2]. Generally, the BHF in conventional deep drawing is applied by counter force, and it is

nonindependent, where flexible and exact control of BHF cannot be obtained. Siegert and Doege [3] proposed a technique utilizing the hydraulics device to apply BHF and can provide a more robust forming process. The hydraulic blank holding equipment was mounted on press, and the variable BHF control was realized. Gunnarsson [4] developed a blank holding system with degressive gas springs, and this system was integrated with the tool body instead of the press. The advantage with this approach is that the system is independent of press facilities, and the BHF can be controlled with the better precision. Thiruvardchelvan and Tan [5] designed a setup in which the BHF and the counter force were provided by hydraulic pressure separately and controlled individually. In this case, the BHF can be adjusted with punch stroke to enhance draw ratio. A new technique on friction aided deep drawing was developed by Hassan [6, 7], in which a blank holder divided into several segments was used instead of rubber ring used in previous process. The blank holder was composed of two layers where the stationary layer was adopted

✉ Siji Qin
plastics@ysu.edu.cn

¹ College of Mechanical Engineering, Yanshan University, 438 West of Hebei Avenue, Qinhuangdao 066004, China

² College of Environment and Chemical Engineering, Yanshan University, Qinhuangdao 066004, China

an integral structure, and moving upper layer was divided into several tapered segments. Every independent segment can move radially to the die opening to obtain appropriate forces at different conditions. Constantly adjusting the moving layer can be employed to increase metal forming limit and assure the dimensional accuracy in forming process.

Due to the hysteresis characteristic of pneumatic transmission and hydraulic systems, the real-time control of BHF is weakened in the techniques mentioned above. In addition, special auxiliary systems with higher costs and relatively complicated operation are also needed in these techniques. In order to improve the real time and effectiveness of BHF control, magnetic force between electromagnet and blank holder was used to supply BHF in the technique proposed by Seo [8]. There are some advantages such as the flexibility and accuracy for BHF control, since the coil current can be changed easily. Huang [9] and Paesea [10] have also studied on electromagnetic technique in sheet metal forming process. However, electromagnetic field can only be generated when the current flow through the coil turns, and disappeared once power off.

The enhancement of magnetic force can be obtained by more coil turns or higher current strength. Thus, lots of heat will be released during applying BHF or forming force in forming process, and energy consumption is large too. These shortcomings of electromagnetic technology restrict their broader practicable application in sheet forming.

The electropermanent magnet (EPM) technology invented by Tecnomagnete S.p.A. has been used in many industrial applications, such as magnetic clamping fixture in manufacturing proposed by Abele [11], memory motors proposed by Magri [12] and Refaie [13], and other related applications. Furthermore, Faranda and Lazzaroni [14] proposed a low-cost temperature measurement in permanent electromagnetic platens. We [15] have proposed a novel BHF technique based on EPM technology in deep drawing process. By this new technique, the BHF can be applied independently by magnetic force which is provided by permanent magnet rather than electromagnet. So there is no impressed current required for maintaining the magnetic field during deep drawing process. Consequently, EPM blank holder technique has both advantages of the electromagnetic blank holder technique and low energy consumption.

2 EPM blank holder technique and design of setup

2.1 Principle of blank holder technique based on EPM

Figure 1 shows a schematic diagram of BHF applied by a counter force in conventional deep drawing process. Generally, a forming process can be regarded as a quasi-static problem, so Eq. (1) can be obtained according to the condition of equilibrium:

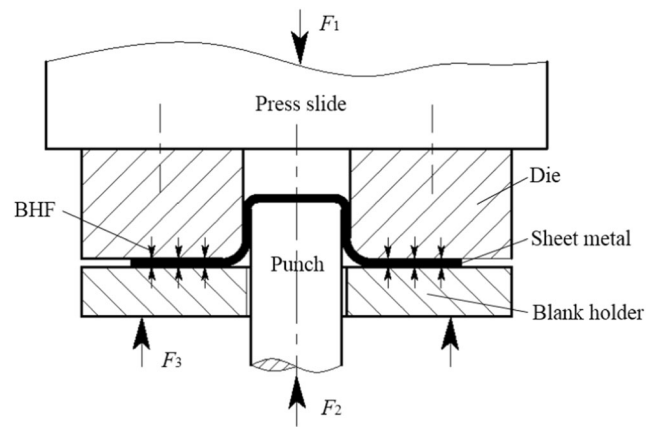


Fig. 1 Deep drawing using conventional blank holder

$$F_1 = F_2 + F_3 \quad (1)$$

where F_2 is forming force of the sheet, F_3 is counter force to maintain the required BHF, and the sum of these two forces should be balanced by the force F_1 applied by the press slide. Because the relative displacement along vertical direction between the blank holder and the die is small due to small change in thickness of the sheet during deep drawing, the energy required for BHF should be very small. However, the actual consumed energy is very large in order to maintain BHF in deep drawing using conventional blank holder. In fact, the energy consumed during applying the BHF in deep drawing is mainly used for the work done by the applied counter force. In view of energy consumption, it is unreasonable to apply BHF using conventional blank holder.

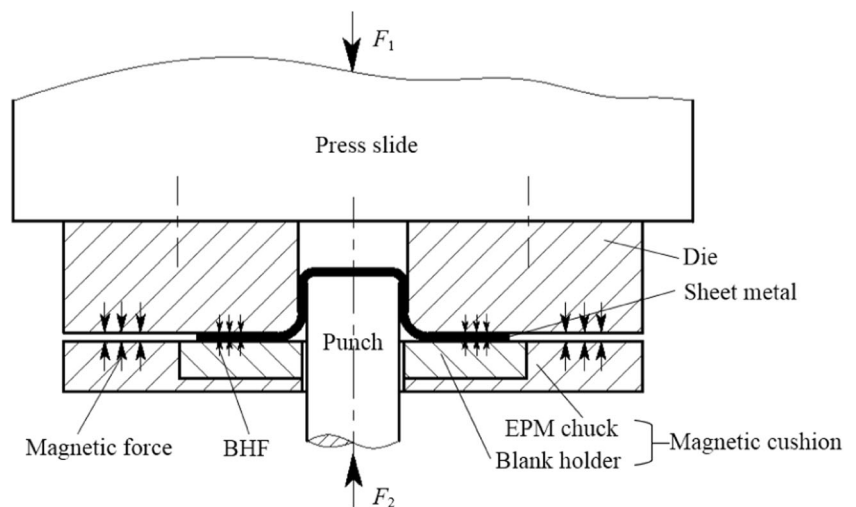
Figure 2 is a schematic diagram of the BHF technique based on EPM. The working state of the magnetic cushion including EPM chuck integrated with blank holder can be changed from one magnetization state to another state or demagnetization state by applying short high-current pulses through the coil windings. As can be seen from Fig. 2, in the case of magnetization state, the EPM chuck is magnetized to generate magnetic force between the chuck and the die. According to the principle of force balance, the magnetic force is equal to the BHF. Because the magnetic force is the internal force of the setup, the unnecessary energy consumption for maintaining counter force (F_3 in Fig. 1) can be avoided by this new technique.

According to the condition of static equilibrium, Eq. (2) can be obtained:

$$F_1 = F_2 \quad (2)$$

Therefore, the F_1 in Fig. 2 is much smaller than that in Fig. 1 according to Eq. (1) and Eq. (2) for the same forming part, so the required tonnage and installed power of the press can be reduced in a great extent.

Fig. 2 Deep drawing using EPM blank holder technique



As shown in Fig. 2, compared with the conventional blank holder, there are many advantages using EPM blank holder technique. Because the magnetic force and the resulting BHF are applied by permanent magnets rather than electromagnets, and the current is only required at the moment of loading or adjusting the BHF. Therefore, there is very low energy consumption during deep drawing process. There is no energy consumption for the BHF while it results from constant magnetic field due to running in power-off state. Based on the same reasons, loss of excitation will not occur in EPM technology even if in the case of power-off accident, and both the reliability and safety of the new technique are very high. Also, the EPM blank holder technique is convenient in control and easy in simplifying tool structure of deep drawing. Therefore, it can be further used to retrofit existing press for in-process control of BHF and be executed automatically in forming production.

In the other hand, because of little temperature rise and without overheating problem and many other advantages, the EPM technology will be more widely used in forming industry.

2.2 Setup using EPM blank holder technique

The designed setup of deep drawing using EPM blank holder technique is shown in Fig. 3. Both the die and the suction plate are mounted on the upper base. The magnetic cushion including EPM chuck integrated with blank holder can provide magnetic force between the chuck and the suction plate and the resulting BHF applied on the sheet metal. The two nitrogen springs are only used for supporting the weight of magnetic cushion, and they do almost no contribution to the BHF during deep drawing.

As shown in Fig. 3, the drawing process using EPM blank holder technique can be described as follows.

Firstly, the upper part of the setup moves down with the slide. The EPM chuck is magnetized by applying short current pulses while the die is in contact with the sheet metal. Then there are closed magnetic circuits constituted between the magnetic cushion and the suction plate, and the resulting magnetic force attracts them each other. In this way, the sheet metal is held tightly between the blank holder and the die while the magnetic force is large enough. As the press slide continues to move downward and the sheet metal touches the punch, the forming begins.

Secondly, the forming process is over when the press slide reaches the bottom dead point, and then the slide and the upper part of the setup start to return. Because of the magnetic force, the magnetic cushion and the drawn part move upward together with the upper part of the setup too. In the meantime, the drawn part is gradually separated from the punch. When the drawn part is about to be completely separated from the punch, the EPM chuck is demagnetized by applying reverse current pulses, and there is almost no magnetic force between the magnetic cushion and the suction plate. Due to the joint action of the limit of the stripper bolts and the ejecting force of the nitrogen springs, the magnetic cushion stops at a certain position, and the drawn part is completely separated from the punch while the slide continues its upward movement.

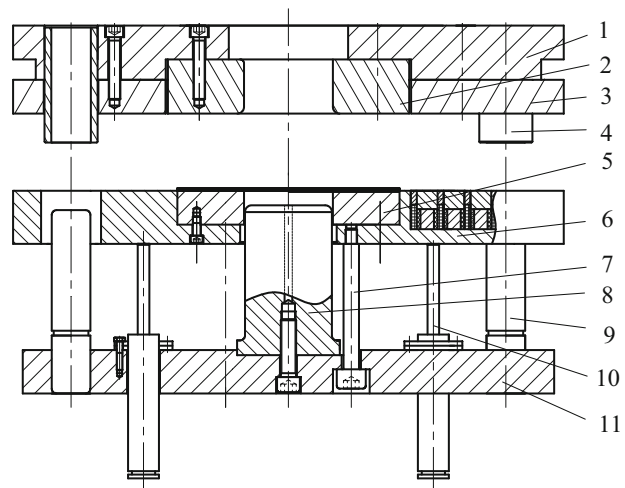
3 Configuration of the magnetic cushion and analysis by FEM

3.1 Working principle of the magnetic pole units and magnetic analysis by FEM

3.1.1 Working principle of the magnetic pole units

In order to illustrate the basic principle of magnetization and demagnetization, a pair of magnetic pole units is taken from

Fig. 3 Schematic diagram of experimental setup using EPM blank holder technique. 1 upper base, 2 die, 3 suction plate, 4 guide bushing, 5 blank holder, 6 EPM chuck, 7 stripper bolt, 8 punch, 9 guide pillar, 10 nitrogen spring, and 11 lower base



1 Upper base, 2 Die, 3 Suction plate, 4 Guide bushing, 5 Blank holder, 6 EPM chuck, 7 Stripper bolt, 8 Punch, 9 Guide pillar, 10 Nitrogen spring, 11 Lower base

the designed magnetic cushion, as shown in Fig. 4. A magnetic pole unit consists of magnetically hard material Nd-Fe-B, semi-hard material Al-Ni-Co, magnetic conductor, and coil. The Nd-Fe-B and the magnetic conductor are placed in the upper part of magnetic pole unit. Nd-Fe-B with high coercivity and high remanence has been recognized to be a better material for large spontaneous magnetic field, and it is used as permanent magnet (PM) here because of constant polarity. Industrial pure iron with high magnetic permeability and high saturation magnetic flux density is used as magnetic conductor for passing magnetic fluxes. In the lower layer, Al-Ni-Co with very low coercivity and high remanence characteristics is used as reversible magnets (RM) because it can provide a powerful magnetic field and easy to switch its polarities. The coils are wrapped on the outside of the Al-Ni-Co. The voids inside the

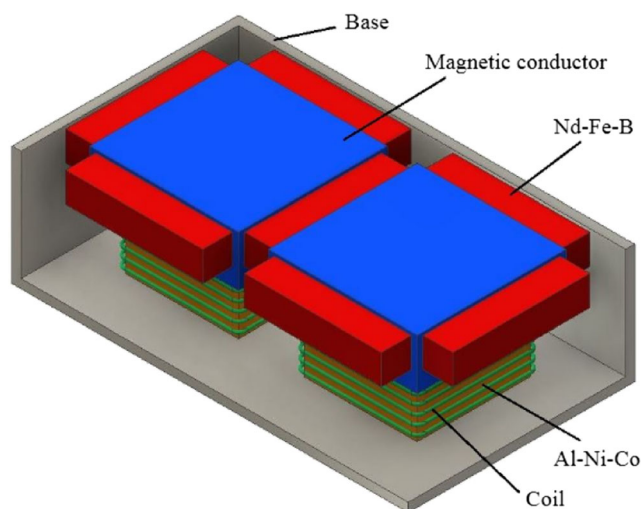


Fig. 4 A pair of magnetic pole units

magnetic pole unit are filled with epoxy resin to increase the integral strength and rigidity and prevent external impurities. The base made of silicon steel can also be used as a magnetic yoke to guide a part of magnetic fluxes to pass through.

An external magnetic field can be generated by applying short current pulses through the coils. This external magnetic field should be strong enough to modify the magnetic field (strength and direction) of RM. Based on the characteristics of PM and RM, the mechanisms of magnetization and demagnetization of magnetic pole unit are described as follows:

- (1) Figure 5a shows the magnetization/loading state of the magnetic pole units. There is a small air gap between the magnetic pole units and the suction plate. In this state, the adjacent poles of PM and RM are modified as the same polarities (*N-N* and *S-S*) by applying short current pulses through coils. The closed magnetic circuits are constituted because the fluxes generated by the magnets exit from poles *N* to poles *S*, and most of fluxes pass through the magnetic conductor, air gap, and suction plate in sequence. The magnetic force between the magnetic pole units and suction plate can be up to highest physical limit as needed. So doing, it is possible to maximize the magnetic flux density of magnetic pole units and attract the suction plate tightly.
- (2) Figure 5b shows the demagnetization/unloading state of the magnetic pole units. The magnetic pole polarities of RM are reversed by applying reverse current pulses. In this state, the adjacent poles of PM and RM are modified as the opposite polarities. Almost all of fluxes pass magnetic pole units themselves from poles *N* of PM to poles *S* of RM or from the poles *N* of RM to the poles *S* of PM by selecting appropriate parameters. In this case, there

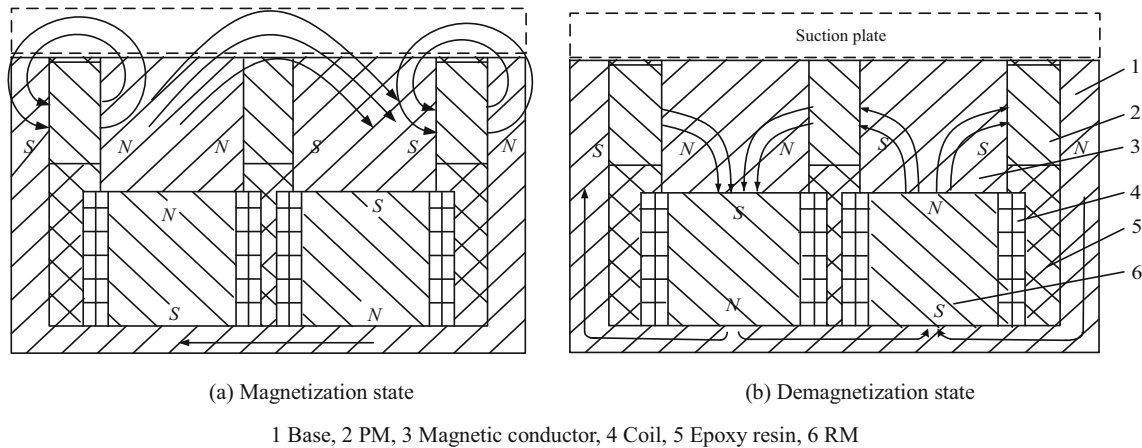


Fig. 5 Magnetic pole units in magnetization and demagnetization states. 1 base, 2 PM, 3 magnetic conductor, 4 coil, 5 epoxy resin, 6 RM

are very few fluxes passing through the suction plate, and the magnetic force between the magnetic pole units and the suction plate is close to zero.

3.1.2 Magnetic analysis of the pole units by FEM

In order to verify the states of magnetization and demagnetization of the magnetic pole units, finite element simulation is carried out by ANSYS software. The magnetic flux density distribution is shown in Fig. 6. It can be seen in Fig. 6a that most of magnetic fluxes pass through the bottom surface of the suction plate in the magnetization state where the average magnetic flux density is about 1.48 T, and the consequent magnetic force is 6709 N. Figure 6b shows the magnetic flux density of magnetic pole units in the demagnetization state. In this state, most of magnetic fluxes pass through the magnetic pole units themselves. The average magnetic flux density on the bottom surface of the suction plate is 0.02 T with a corresponding magnetic force of 3 N.

The simulated results show that the magnetization and demagnetization can be realized by this magnetic circuit design.

3.2 Configuration of the magnetic cushion and analysis by FEM

3.2.1 Configuration of the magnetic cushion

In order to obtain sufficient magnetic force and resulting BHF, and consider that the setup may be used in other forming process such as bulging (just replace some forming tools), the horizontal size of the magnetic cushion is designed to be larger than the actual need. In contrast, the horizontal size of blank holder is designed to be slightly smaller.

According to the electromagnetic field theory, the magnetic flux density B_g in the air gap between the magnetic poles and the suction plate can be estimated by Eq. (3):

$$B_g = H_m S_m / (\mu_0 S_g K_f) \tag{3}$$

where H_m is the magnetic field strength of the pole units, S_m and S_g are the cross-sectional areas of the magnetic pole units and air gap, respectively, μ_0 is the permeability of vacuum, and K_f is the magnetic leakage factors.

So, in the design of magnetic cushion, the material, shape, size, number of magnetic pole units, and other parameters of the structure should be taken into consideration. Figure 7 shows the cutaway view of the designed EPM chuck.

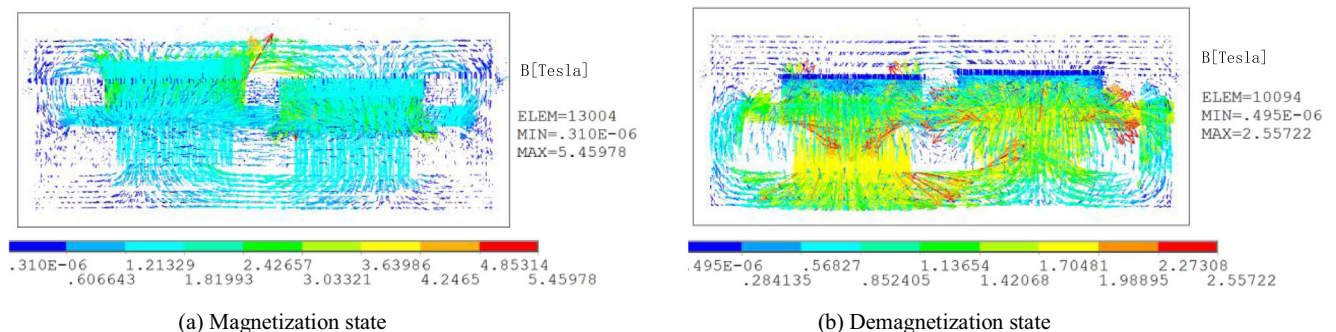


Fig. 6 Magnetic flux density distribution of magnetic pole units

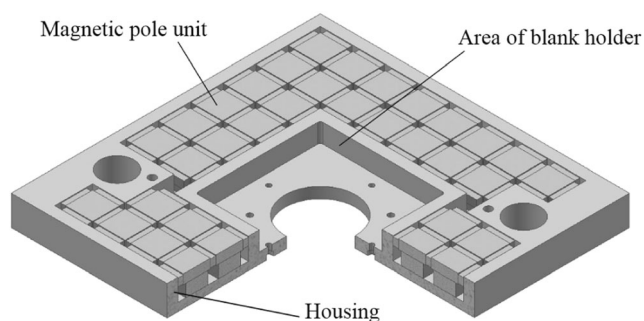


Fig. 7 Schematic diagram of EPM chuck

The dimensions of the designed magnetic cushion are 570 mm × 570 mm × 57 mm, and the sizes in the horizontal plane of the blank holder are 230 mm × 230 mm. The blank holder can be replaced according to forming processes of the sheets with different thickness. There are a total of 46 magnetic pole units placed in the cushion. The magnetic pole units include 46 pieces Al-Ni-Co (38 mm × 38 mm × 15 mm), 46 pieces magnetic conductor (50 mm × 50 mm × 17 mm), and 120 pieces Nd-Fe-B (46 mm × 10 mm × 10 mm).

3.2.2 3-D static magnetic analysis by FEM

The static magnetic analysis is carried out by ANSYS, in which a 3-D model including magnetic cushion, air gap, and a 35-mm thick suction plate is established. The air gap between the EPM chuck and the suction plate is set to be close to zero. Materials and their properties used for analysis are shown in Table 1. The Solid98 element allows magnetic scalar potential and displacement to be specified, and then calculation is executed by using magnetic scalar potential algorithm.

Figures 8 and 9 show the magnetic flux density distributions of the magnetic cushion in the states of magnetization and demagnetization, respectively. As shown in Fig. 8, almost all of the magnetic fluxes are distributed on the areas of square magnetic pole units, while the magnetic cushion is adjusted to the maximum magnetization state by applying current pulses. There are almost no magnetic fluxes in other areas. The average magnetic flux density in the air gap and the consequent magnetic force are 1.36 T and 152,598 N, respectively, which are close up to the highest physical limits.

Table 1 Material properties for magnetic field analysis

Components	Materials	Properties	
		Coercivity (kA/m)	Relative permeability
PM	Nd-Fe-B	928	1.05
RM	Al-Ni-Co	59	17.05
Housing	Silicon steel	0	9000
Conductor/die	Pure iron	0	4000
Gap/resin	Air/resin	/	1

As shown in Fig. 9, when the magnetic cushion is adjusted to the demagnetization state by applying reverse current pulses, the average magnetic flux density is 0.01 T, and the total magnetic force is very small (less than 15 N). It shows that the designed magnetic cushion can be demagnetized well.

According to Maxwell's electromagnetic field theory, the magnetic force F between magnetic cushion and suction plate can be estimated by Eq. (4) as follows:

$$F = \frac{\mu_r - 1}{2\mu_0\mu_r} B_g^2 S_g \quad (4)$$

where μ_r is the relative permeability of the suction plate.

It is shown that the magnetic force is mainly affected by the magnetic flux density and the cross-sectional area of the air gap according to Eq. (4). In addition, since the cross-sectional area of the air gap has been given, the magnetic force is mainly determined by the magnetic flux density, which varies with the width of the air gap.

In order to investigate the effect of air gap on the magnetic force in detail, the relationship between the total magnetic force and the width of air gap is analyzed by FEM. The magnetic flux density of the designed magnetic cushion is divided into 16 levels and can be adjusted by applying different current pulses. Figure 10 shows the relationship between magnetic forces and air gaps under four different magnetic field levels, respectively. It is shown that the total force decreases dramatically with the increase of the width of the air gap. The width of the air gap can be changed as needed by adjusting the thickness of the blank holder.

3.2.3 Structural analysis model

The geometric models for analysis include the magnetic cushion, sheet, and the upper part of the setup. The boundary conditions set for analysis are described as follows.

Set the top surface of the upper base as fixed displacement constraint. The values and distributions of the magnetic force determined by magnetic field analysis are used as pressure load and applied on the top surfaces of the pole units of the cushion and corresponding surfaces of the suction plate, respectively. The relationships between the sheet and suction plate, the sheet and the blank holder of the cushion, are defined as contacts, and the nonlinear contact analysis is used in calculation. The materials used in the various parts of the model are assigned to the corresponding properties.

For a given magnetic force and its distribution, the displacement, strain, and stress of the structure can be obtained by FEM.

3.2.4 Analysis of coupling fields

In general, for a coupling problem of structural and magnetic fields, deformation and stress of the structure will be caused

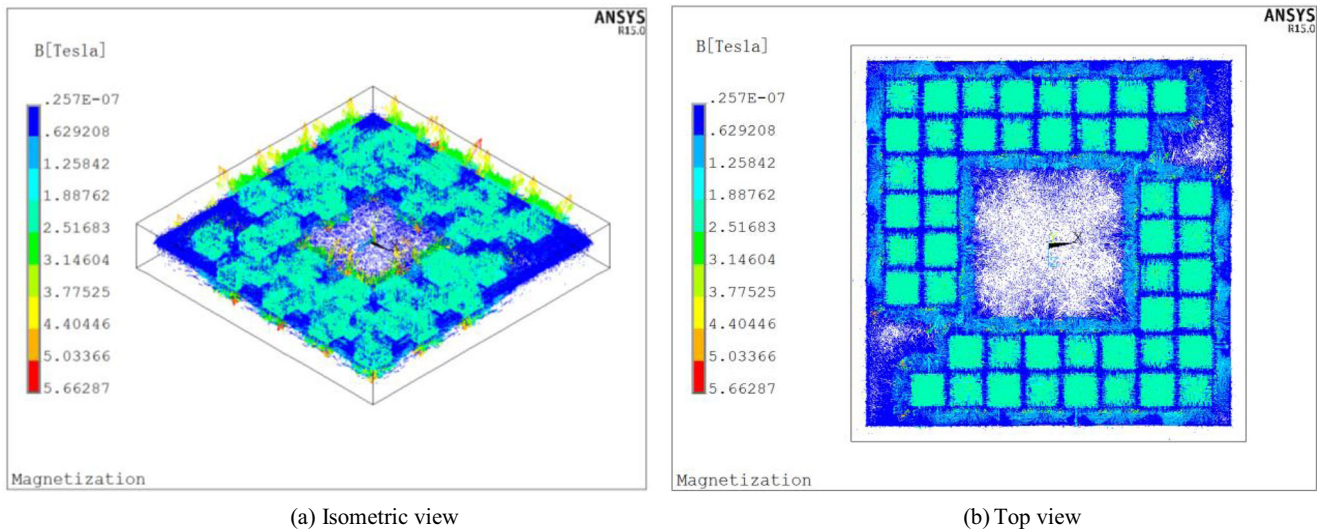


Fig. 8 The magnetic flux density distribution of the magnetic cushion in magnetization state

by magnetic force, while the magnetic force is further affected by the deformed structure.

What we are investigated here is a coupling problem involving structural and magnetic fields. In the magnetization state, the air gap between the suction plate and the magnetic cushion becomes smaller under the applying magnetic force, which is further affected by the change of the air gap in turn.

Considering that the ANSYS software cannot be directly used for the coupling analysis of magnetic force and structure, and in order to understand more detailedly the internal relationship between magnetic force and structural deformation with EPM blank holder technique, the solution of the coupling problem based on FEM is analyzed as follows.

It is assumed that the magnetic forces are applied on the surfaces of the suction plate and the magnetic cushion and are along the vertical direction. The magnitude of a magnetic force at one position of the suction plate is equal to that at

the same position along vertical direction of the magnetic cushion. Let $\{F\}$ be a magnetic force vector, and $\{\delta_0\}$ and $\{\delta\}$ be vectors of the initial air gap and final actual gap, respectively, between the suction plate and the magnetic cushion. Let the relationship between the magnetic force and the air gap be expressed as Eq. (5):

$$\{F\} = \{F(\{\delta\})\} \tag{5}$$

Let $\{\delta_1\}$ be a vertical displacement vector of arbitrary reference positions of the suction plate, and $\{\delta_2\}$ be a vertical displacement vector of the same positions along vertical direction of the magnetic cushion, and $\{\delta_0\}$ and $\{\delta\}$ are further set to the vertical vectors of the same positions of the structure along vertical direction. Therefore, Eq. (6) can be expressed as follows:

$$\{\delta\} = \{\delta_0\} - \{\delta_1\} - \{\delta_2\} \tag{6}$$

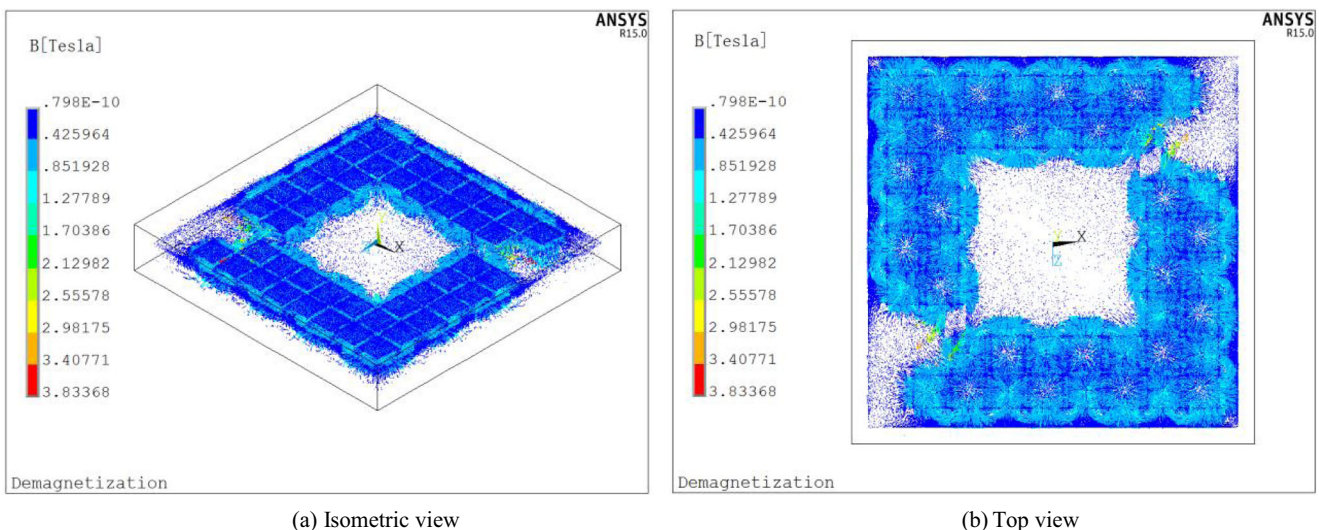


Fig. 9 The magnetic flux density distribution of the magnetic cushion in demagnetization state

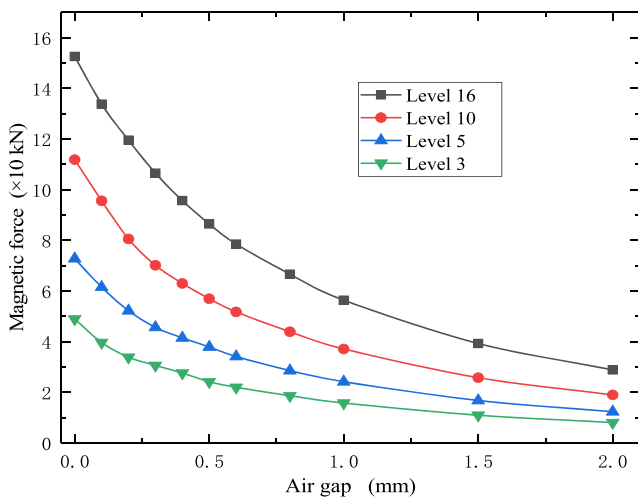


Fig. 10 Magnetic force variations with width of air gap

According to the theory of elastic mechanics, under the assumptions of elasticity and small deformations, displacement of structure is proportional to applied force provided that the direction and position of the force do not change. Let $[K_1]$ be the stiffness matrix of upper part of the setup and $[K_2]$ be the stiffness matrix of the magnetic cushion; the relationships between $\{F\}$ and $\{\delta_1\}$ and $\{F\}$ and $\{\delta_2\}$ can be expressed as Eq. (7) and Eq. (8), respectively:

$$\{F\} = [K_1]\{\delta_1\} \tag{7}$$

$$\{F\} = [K_2]\{\delta_2\} \tag{8}$$

Eq. (9) can be obtained as follows by substituting Eq. (7) and Eq. (8) into Eq. (6):

$$\{\delta\} = \{\delta_0\} - \{F\}[K_1]^{-1} - \{F\}[K_2]^{-1} \tag{9}$$

Thus,

$$\{F\} = [K](-\{\delta\} + \{\delta_0\}) \tag{10}$$

where $[K] = 1/([K_1]^{-1} + [K_2]^{-1})$.

$\{F\}$ and $\{\delta\}$ can be determined by Eq. (5) and Eq. (10) while $[K]$ is constant. In fact, however, the displacement is no longer proportional to the force because the positions of the magnetic forces applied to the structure change during loading process and $[K]$ is not constant. Obviously, it is difficult to solve this problem theoretically due to the complex and nonlinearity of the structure. Generally, the problem should be solved on the basis of theoretical analysis and by means of FEM.

To simplify the analyses of structures and magnetic fields, it is assumed that the vertical displacement of the outer edge of the magnetic cushion surface is the same, so is that of the suction plate surface. The two vertical displacement variables are represented by δ_2 and δ_1 , respectively, as shown in Fig. 11. Let F be the total magnetic force, and δ be the final actual air gap between the outer edges of the suction plate and the

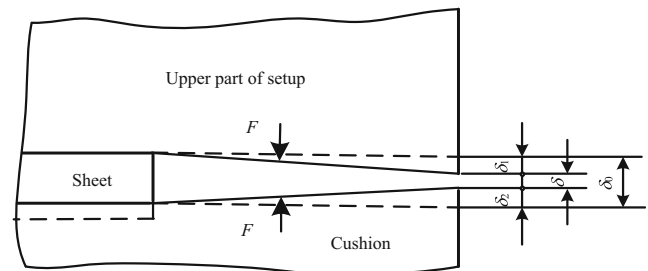


Fig. 11 Schematic diagram of magnetic force and deformation

magnetic cushion. These scalar variables are a special case of the vectors and are still satisfied with the equations from (5) to (10).

As shown in Fig. 11, for simplicity, it is further assumed that displacements of the upper part of the setup and the cushion vary linearly from the outer edge to the support position of the sheet. Let us take several values between 0 and δ_0 and set them equal to δ , respectively, and models of magnetic field can be reconstructed, and the relationship between the magnetic force F and final air gap δ corresponding to Eq. (5) can be obtained by FEM. The relationship between F and δ corresponding to Eq. (10) can also be obtained by FEA of the structure. Obviously, the intersection of the two curves corresponding to Eq. (5) and Eq. (10) is the solution which varies with the magnetic field level and the initial air gap.

As shown in Fig. 12, curve families A, B, C, and D are the relationships between the magnetic force F and final air gap δ based on Eq. (5) obtained by FEM according to Section 3.2.2 under the magnetic field levels 16, 10, 5, and 3, respectively, and different initial air gaps. A1, A2, A3, A4, and A5 are curves of F varied with δ under the initial air gaps 0.1 mm, 0.2 mm, 0.3 mm, 0.4 mm, and 0.5 mm, respectively, and the same magnetic field level, and the curve families B, C, and D have similar meanings.

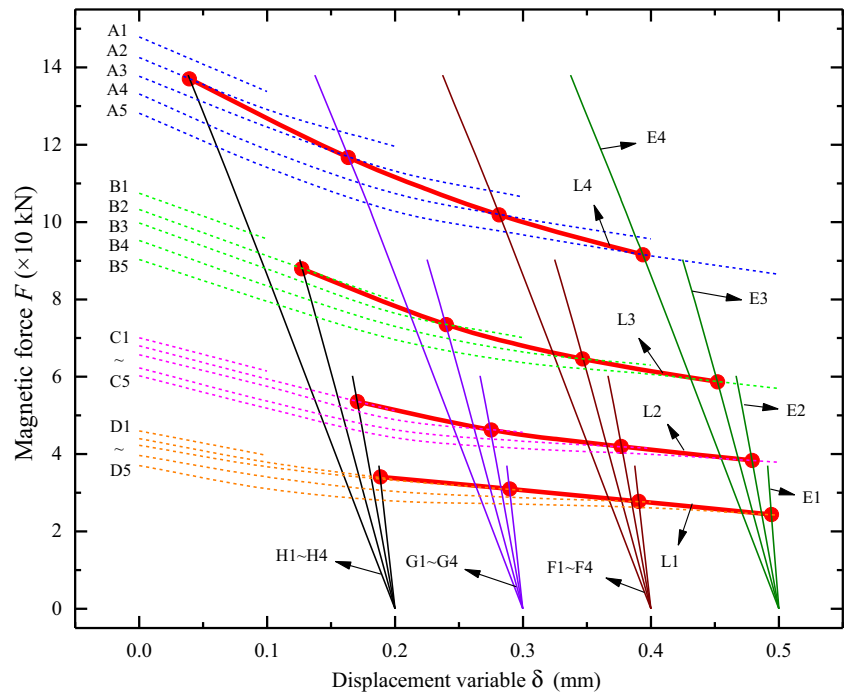
Curve families E, F, G, and H are all curves of F varied with δ based on Eq. (10) under the initial air gaps 0.5 mm, 0.4 mm, 0.3 mm, and 0.2 mm, respectively, and different magnetic field levels according to FE analysis of the structure. E1, E2, E3, and E4 are the relationships between F and δ under the magnetic field levels 3, 5, 10, and 16, respectively, and the same initial air gap, and the curve families F, G, and H have similar meanings.

Thus, a series of solutions under different magnetic field levels and initial air gaps can be obtained. L1, L2, L3, and L4 are lines of solutions under the magnetic field levels 3, 5, 10, and 16, respectively, and different initial air gaps.

According to the curve family L and the given value of the BHF, which is equal to the magnetic force, the required magnetic field level, the initial and the final air gaps, can be obtained by combining the drawing and interpolation methods.

In addition, it can be seen from the analysis results that the mechanical strength of the designed EPM cushion is strong enough, and the stiffness of the setup can satisfy the requirements.

Fig. 12 The magnetic force F varied with displacement variable δ



3.2.5 Blank holding pressure applied by magnetic force

The final magnetic force distribution can be obtained according to the foregoing description while the magnetic field level and the final air gap are given. Then the contact pressure on the sheet can be determined based on the analysis of structure by applying the calculated magnetic force.

Figure 13 shows the distribution of the contact pressure on the sheet while $\delta_0 = 0.5$ mm and the magnetic field level is 5.

The calculated contact pressure on the sheet is the blank holding pressure, which is distributed in a narrow outer area of the sheet along radial direction, as shown in Fig. 13. It is also shown that the distribution of the blank holding pressure is approximately the same along circumferential direction.

Obviously, the blank holding pressure distribution using EPM blank holder technique is different from that using conventional blank holder. In fact, however, the blank holding pressure applied by conventional blank holder is also

distributed in a narrow edge area of the sheet due to the increase of outer edge thickness of the sheet during deep drawing. So, it can be foreseen that the forming effectiveness using the new technique is close to that using conventional blank holder.

4 Simulations and experiments of sheet metal forming

4.1 Simulations

In order to evaluate the effectiveness of deep drawing with conventional blank holder and EPM blank holder technique, respectively, the simulations are performed by DYNIFORM. The material is characterized using the Barlat-Lian 89 yield criterion. Rigid shell elements are used to mesh the tools, including die, blank holder, and punch [16]. Belytschko-Lin-Tsay shell elements are applied to mesh the sheet. The friction type is set as the contact one-way surface-to-surface mode. The relationship between stress and strain is using the Hollomon power-hardening rule. The material properties of 08Al sheet (thickness $t = 0.98$ mm) and tooling parameters are shown in Tables 2 and 3, respectively. According to the estimated blank holding pressure given by Fukui and Yoshida [17] and previous experience, set the BHF equal to 38.3 kN (corresponding to the magnetic field level 5 and the initial air gap 0.5 mm) for the selected blank sheet, and set it equal to the magnetic force. Take the same applied BHF using conventional blank holder and EPM blank holder technique, respectively,

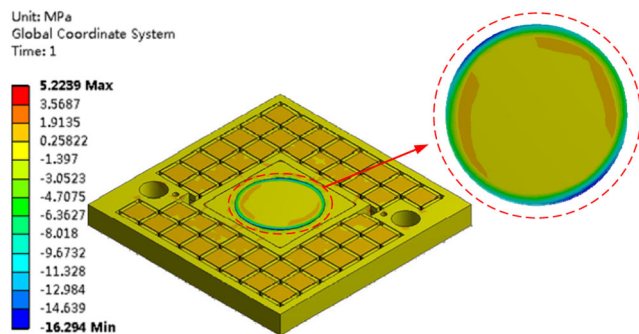


Fig. 13 The results of blank holding pressure

Table 2 Material properties of 08Al sheet

Parameters	Values
Strain hardening exponent	0.23
Strain hardening coefficient	595 MPa
Normal anisotropy parameter	1.86
Young's modulus	215 GPa
Poisson's ratio	0.30
Mass density	7.85 g/cm ³
Yield strength	270 MPa
tensile strength	345 MPa

in deep drawing, but the blank holding pressures are different. The method to determine the distribution of blank holding pressure by the EPM technique is described in Section 3.2.5.

Figure 14 shows the strain distributions of the drawn parts while the drawing depth is 50 mm, where R_0 is the initial sheet radius and r is the initial position radius of the element of the sheet. The results show that under the condition of the same total blank holder force but different initial blank holding pressure, there are small differences of the strain distributions of the drawn parts with the two blank holders, respectively. In other words, the forming effect using the EPM blank holder is close to the conventional blank holder.

4.2 Experiments

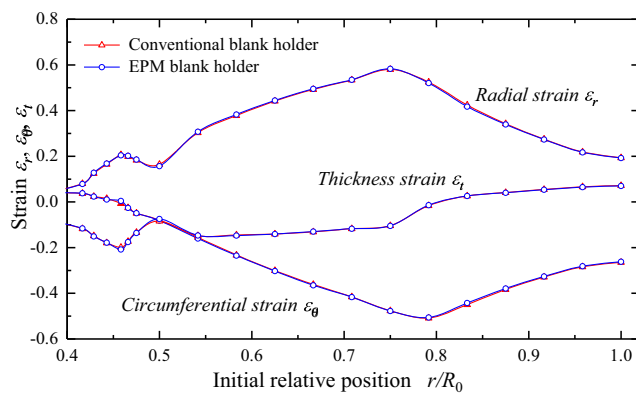
As shown in Fig. 15, the experimental setup designed in Section 2.2 was built, and the magnetic flux density generated by the magnetic cushion was divided into 16 levels and can be controlled by a controller.

A set of experiments were performed to validate the actual effect of the EPM blank holder technique. The parameters of the selected sheet and drawing tools are the same as those used in FEA.

Examples of drawn cups applying BHF by using EPM blank holder technique at different levels of magnetic flux density are shown in Fig. 16a–d, respectively. All drawn cups were obtained with the same stroke of the press slide and the maximum forming height is about 45 mm. As shown in Fig. 16a, there is severe wrinkling on the flange of drawn cup due to an insufficient BHF while the magnetic flux density was set to a smaller value, level 1. And the wrinkling can

Table 3 Tooling parameters

Parameters	Values (mm)
Sheet diameter	190
Punch diameter	90
Punch arc radius	5.0
Die diameter	92.5
Die arc radius	5.0

**Fig. 14** Strain distributions of the drawn part by FEM

be reduced significantly applying greater BHF while the magnetic flux density was increased to level 2, as shown in Fig. 16b. A successful drawn cup without wrinkling shown in Fig. 16c was obtained when the magnetic flux density was further increased to level 5 while the BHF is enough to prevent wrinkling. However, as the BHF continued to increase, a fracture occurred during deep drawing when the magnetic flux density was level 10, as shown in Fig. 16d.

As can be seen from experimental results, the maximum magnetic force and resulting BHF provided by magnetic cushion is much larger than the required for the selected sheet. That is, the sizes of the designed magnetic cushion and some other components can be greatly reduced for the forming of the selected sheet blank.

5 Discussion and conclusions

The feasibility of the EPM blank holder technique has been verified by simulations and experiments. Many technical and



1 Press slide, 2 Upper base, 3 Suction plate and die, 4 Blank holder, 5 EPM chuck, 6 Controller, 7 Punch, 8 Nitrogen spring, 9 Lower base

Fig. 15 Experimental setup. 1 press slide, 2 upper base, 3 suction plate and die, 4 blank holder, 5 EPM chuck, 6 controller, 7 punch, 8 nitrogen spring, 9 lower base

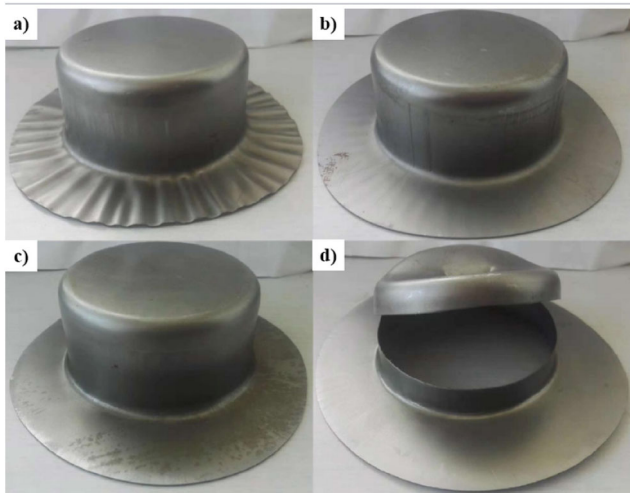


Fig. 16 Drawn cups using EPM blank holder technique with different magnetic flux density levels: **a** Level 1, **b** Level 2, **c** Level 5, and **d** Level 10

economic advantages using this new technique are also discussed in the present paper. It should be mentioned that a better performance of EPM blank holder technique can be obtained by improving structure of tools and better control technology. These should be done as future work on the present process.

Taken together, we can come to the conclusions as follows:

- (1) The work presented in this paper proposes a novel blank holder technique to be implemented in sheet forming. EPM blank holder technique not only inherits the advantages of the previously proposed independent loading methods based on electromagnet technologies but also overcomes some of their deficiencies.
- (2) The FE simulations of deep drawing are performed under the blank holding pressure applied by magnetic force using EPM blank holder technique. The forming effective using the EPM blank holder is close to the conventional blank holder.
- (3) The deep drawings of cylindrical cups have been experimented applying different BHF, and the results show that EPM blank holder technique used in deep drawing is feasible, and the BHF applied by magnetic force can be large enough required for the selected sheet.
- (4) The mechanical strength of the designed EPM cushion is strong enough, and the stiffness of the setup can satisfy the requirements. The temperature rise of the EPM cushion is low and without overheating problem during applying the BHF in deep drawing. The EPM blank holder technique will be expected to be used to retrofit the forming processes and design new types of presses.

Funding Information The authors are pleased to acknowledge the financial support of National Natural Science Foundation of China (Nos. 51675466 and 51175451). The work is also supported by the Natural Science Foundation of Hebei Province of China (No. E2018203373).

References

1. Obermeyer EJ, Majlessi SA (1998) A review of recent advances in the application of blank-holder force towards improving the forming limits of sheet metal parts. *J Mater Process Technol* 75(1/3):222–234
2. Irthia IK, Green G (2017) Evaluation of micro deep drawing technique using soft die-simulation and experiments. *Int J Adv Manuf Technol* 89:2363–2374
3. Siegert K, Doege E (1993) CNC hydraulic multipoint blankholder system for sheet metal forming presses. *CIRP Ann Manuf Technol* 42(1):319–322
4. Gunnarsson L, Asnafi N, Schedin E (1998) In-process control of blank holder force in axi-symmetric deep drawing with degressive gas springs. *J Mater Process Technol* 73(1/3):89–96
5. Thiruvarduchelvan S, Tan MJ (2007) Fluid-pressure-assisted deep drawing. *J Mater Process Technol* 192–193:8–12
6. Hassan MA, Takakura N, Yamaguchi K (2003) Friction aided deep drawing using newly developed blank-holder divided into eight segments. *Int J Mach Tools Manuf* 43(6):637–646
7. Hassan MA, Suenaga R, Takakura N, Yamaguchi K (2005) A novel process on friction aided deep drawing using tapered blank holder divided into four segments. *J Mater Process Technol* 159(3):418–425
8. Seo YR (2008) Electromagnetic blank restrainer in sheet metal forming processes. *Int J Mech Sci* 50(4):743–751
9. Huang YJ, Han XT, Cao QL, Lai ZP, Cai H, Liu N et al (2017) Design and analysis of a pulsed electromagnetic blank holder system for electromagnetic forming. *Procedia Eng* 207:347–352
10. Paesea E, Geierb M, Homrich RP, Rosad P, Rossie R (2019) Sheet metal electromagnetic forming using a flat spiral coil: Experiments, modeling, and validation. *J Mater Process Technol* 263:408–422
11. Abele E, Altintas Y, Brecher C (2010) Machine tool spindle units. *CIRP Ann Manuf Technol* 59(2):781–802
12. Magri AE, Giri F, Abouloifa A, Chaoui FZ (2010) Robust control of synchronous motor through AC/DC/AC converters. *Control Eng Pract* 18(5):540–553
13. EL-Refaie AM (2010) Fractional-slot concentrated-windings synchronous permanent magnet machines: opportunities and challenges. *IEEE Trans Ind Elect* 57(1):107–121
14. Faranda R, Lazzaroni M (2013) Industrial low cost temperature measurement in permanent electro-magnetic platens. *Measurement* 46(1):324–335
15. Qin SJ, Wang GZ, Ma YF, Kong XH, Deng C (2015) Deep drawing tool with blank holder technique based on electro permanent magnet technology. No. CN 1094040A (in Chinese)
16. Tseng HC, Hung CH, Huang CC (2010) An analysis of the formability of aluminum/copper clad metals with different thicknesses by the finite element method and experiment. *Int J Adv Manuf Technol* 49:1029–1036
17. Fukui S, Yoshida K (1954) The scale effects on deep-drawing of circular shells. *R Ins Sci Technol, Univ Tokyo* 8:23–30

Publisher's note Springer Nature remains neutral with regard to jurisdictional claims in published maps and institutional affiliations.